Brazilian Dental Science

unesp
UNIVERSIDADE ESTADUAL PAULISTA
"JÚLIO DE MESQUITA FILHO"
Instituto de Ciência e Tecnologia
Campus de São José dos Campos

ORIGINAL ARTICLE

DOI: https://doi.org/10.4322/bds.2024.e4356

The optical behavior of pressable lithia-based glass-ceramics under two different heat treatment protocols

O comportamento óptico de vitrocerâmicas prensadas à base de lítio sob dois protocolos diferentes de tratamento térmico

Iman Haggag Elnagar AHMED[1], Amr EL-ETREBY[2,3], Sara Mehanna FOUDAH[2]

1 - October 6 University, Faculty of Dentistry, Fixed Prosthodontics. Cairo, Egypt.
2 - Ain Shams University, Faculty of Dentistry, Fixed Prosthodontics. Cairo, Egypt.
3 - Tallinn Health Care College. Tallinn, Estonia.

How to cite: AHMED IHE, El-Etreby A, Foudah SM. The optical behavior of pressable lithia-based glass-ceramics under two different heat treatment protocols. Braz Dent Sci. 2024;27(2):e4356. https://doi.org/10.4322/bds.2024.e4356

ABSTRACT

Objective: This study aimed to evaluate the optical behavior of pressable lithia-silicate and lithia-zirconia-silicate glass ceramics toward additional heat treatment protocols. **Material and Methods:** 40 lithia-silicate discs (15mm x 1mm) were heat pressed following the manufacturers' instructions. Discs were divided into four groups (n=10) according to type as follows: two groups of lithia-silicate-glass ceramics; Gp(E) (IPS e.max Press; Ivoclar Vivadent AG), Gp(L) (GC Initial LiSi Press, GC), two lithia-zirconia-silicate pressable glass ceramics; Gp(C) (Celtra Press, Dentsply Sirona) and Gp(A) (VITA Ambria, VITA Zahnfabrik). Each group was subdivided into (n=5): Subgroup(T1): the thermal tempering temperature was set 9% below the pressing temperature, Subgroup(T2): the temperature was set 5% below the pressing temperature. Optical properties: color, translucency parameter (TP), and contrast ratio (CR) were evaluated by spectrophotometer (Aglient Cary 5000 UV-Vis–NIR) after pressing and after thermal tempering. **Results:** Thermal tempering regardless of temperature resulted in a color shift within the acceptability level as ΔE for Gp(E) (3.18±2) followed by ΔE for Gp(L) (2.47±0.19) by ΔE for Gp(C) (2.26±0.14) and the last ΔE for Gp(A) (1.62±0.13). Subgroup(T2) showed a significantly higher color shift with mean ΔE(2.55±0.63) compared to Subgroup(T1) ΔE(2.35±0.59). There was a statistically significant increase in TP after tempering for all tested groups parallelled with a decrease in CR values. **Conclusion:** Heat tempering of the tested lithia-silicate pressable ceramics had a significant effect on the optical outcome of these materials, being lithia-zirconia-silicate ceramics more stable and less affected optically than other lithia-silicate-glass ceramics.

KEYWORDS

Ceramics; Glass ceramics; Hot temperature; Silicates; Zirconium oxide.

RESUMO

Objetivo: Avaliar o comportamento óptico de cerâmicas pressionáveis de vidro de litia-silicato e litia-zircônia-silicato sob protocolos adicionais de tratamento térmico. Materiais e métodos: 40 discos de litia-silicato (15mm x 1mm) foram prensados a quente conforme instruções dos fabricantes. **Material e Métodos:** 40 discos de litia-silicato (15mm x 1mm) foram prensados e divididos em quatro grupos (n=10): dois de lithia-silicato-vidro, Gp(E) (IPS e.max Imprensa) e Gp(L) (GC inicial LiSi Press), e dois de vidro prensado de litia-zircônia-silicato, Gp(C) (Celtra Press) e Gp(A) (VITA Ambria). Cada grupo foi subdividido em (n=5): Subgrupo(T1): amostras temperadas a 9% abaixo da temperatura de prensagem, e Subgrupo(T2): a temperatura foi ajustada 5% abaixo da temperatura de prensagem. As propriedades ópticas, incluindo cor, translucidez (TP) e contraste (CR), foram avaliadas com um espectrofotômetro (Aglient Cary 5000 UV-Vis-NIR) após prensagem e temperagem térmica. **Resultados:** O tratamento térmico resultou em mudança de cor dentro do nível aceitável, com ΔE mais alto para

Gp(E) (3,18±2), seguido por Gp(L) (2,47±0,19), Gp(C) (2,26±0,14), e Gp(A) (1,62±0,13). No subgrupo (T2), houve uma mudança de cor mais significativa, com ΔE médio de (2,55±0,63), comparado ao subgrupo (T1) com ΔE médio de (2,35±0,59). Houve aumento significativo na TP e redução nos valores de RC após o tratamento térmico em todos os grupos testados. **Conclusão:** O tratamento térmico das cerâmicas prensadas de litia-silicato teve um efeito significativo na sua qualidade ótica, com as cerâmicas de litia-zircônia-silicato mostrando-se mais estáveis e menos afetadas visualmente em comparação com outras cerâmicas de litia-silicato-vidro.

PALAVRAS-CHAVE

Cerâmica; Cerâmica de vidro; Temperatura quente; Silicatos; Óxido de zircónio.

INTRODUCTION

Lithium silicate-based ceramics (LSCs) stand out among the many all-ceramic materials that have entered the dental market in recent years and have the potential to establish themselves as the preferred choice, particularly for single restorations [1,2]. Dental manufacturers have frequently attempted to combine mechanical efficiency and aesthetic quality, making lithium silicate materials an exemplar that meets both requirements [3]. The introduction of such materials that are effectively used in monolithic mode rendered the necessity for bilayer restoration redundant [4]. Nevertheless, these materials were produced in a versatile manner using the well-known earlier heat pressing technology or the following digital production using CAD/CAM, which made them tempting and easy to use [5]. A material with visual qualities comparable to glass ceramics and superior mechanical performance was a revolutionary breakthrough when it was first introduced to the dental market in the 1990s as IPS Empress II (Ivoclar Vivadent, Schaan, Liechtenstein) utilizing the hot-press technology [6,7]. The next generation was around 2001 with the release and patenting of IPS e.max Press (Ivoclar Vivadent, Schaan, Liechtenstein) [8]. This moldable version utilized the lost wax technology based on the viscous flow of glass-ceramics with the advantages of net-shape processing, decreased porosity, increased Weibull modulus, increased flexural strength, and providing excellent marginal fit [9]. Early around the year 2005 the introduction of IPS e.max CAD® (Ivoclar Vivadent, Schaan, Liechtenstein) [10], took place as the machinable CAD/CAM version for the chair side delivery of such restorations utilizing the digital workflow. These moldable and machinable glass-ceramics that precipitate lithium disilicate have been utilized to create more than one hundred eight million dental restoration pieces over 8 years of exclusive presence in the dental market with recorded excellence of clinical durability [11,12]. This encouraged producers and scientists to continue developing this kind of material to increase its potential applications, especially once the material's patent expired. In 2013 just after the launching of a second lithium silicate-based ceramic material by Glidewell Laboratories [13], reinforcements of these materials by adding zirconia to its chemical structure was pioneered by lithia-zirconia silicate glass ceramics such as Celtra Duo (Dentsply Sirona, York, PA, USA) and Suprenity PC (Vita Zahnfabrik, Bad Säckingen, Germany) with addition of around 8-12% zirconium oxide to the structure. The trend of creating novel lithia silicates with reducing crystal dimensions while maintaining around 50 vol% crystallinity - to aid in millability and subsequent processing capability - is being driven by the inclusion of ZrO2 as an auxiliary nucleate center [14]. This resulted in lithium (mono)-silicate crystals and the presence of biphasic variants with lithium meta-silicate and lithium disilicate is evident [15]. Variations in the manufacturing techniques and different microstructural forms of the material were noticed to have consequences for the final material properties [15]. Heat application is an essential process required during the whole process of manufacturing. Starting with the early preprocessing stages of ingot fabrication and reaching the further treatments involved to create the final tooth-shaped restoration [6,15,16]. An essential second round of heat application at the laboratory level is needed as follows; for moldable versions, these ingots are being subjected to high pressing temperature dictated by the manufacturer at the dental lab. Typically, machinable versions are supplied in a pre-crystallized state that eases the machinability but needs an essential crystallization firing cycle. Additional third levels of firing cycles may be recommended for some esthetic characterizations, corrections, glazing, or healing and reinforcements. These tuning procedures with variable temperatures, heating rates, holding times,

or cooling rates have been evidenced to affect the material structure, crystallization formation, and growth [17]. Consequently, the mechanical, and physical impacts of such treatments were reported in the literature with controversial conclusions. While some discussed how applying heat can elevate internal stresses [18,19], affecting the strength negatively [18,20], and increasing the chairside time with post-processing additional firings required, others have noted that it can also have a strengthening impact [21,22]. While speed firing has been attempted to facilitate crystallization [23], prefacing of such lithia-silicate based restoration was introduced so that restorations could be milled, polished, and delivered with the elimination of the post-mill crystallization firing needed and substitution by a minor post-mill glaze firing that inherently heals any machining flaws like in Cerec Tessera (Dentsply Sirona, York, PA, USA). Moreover grinding fully crystallized materials without any post-grind heat treatment was finally introduced with the launching of materials such as GC Initial LiSi Block (GC, Tokyo, Japan) [24], and N!CE (Straumann, Basel, Switzerland) [25]. On the other hand, manufacturers reported an increase of about 160 MPa in flexural strength for the LSCs subjected to an additional firing cycle over that of the machined one [26]. Not only for mechanical benefit, optical optimization for the translucency level of a material like Amber mill (HASSBio, Kangneung, Korea) [27], was recommended by the manufacturer through changing the temperature of the crystallization cycle. For a recently introduced lithia-zirconia silicate ceramic in 2021, VITA Ambria (VITA Zahnfabrik, Bad Säckingen, Germany) [28], an additional third step of heat tempering at 800 °C is recommended by the manufacturer to increase the strength of the pressed restorations [29]. The effect of such heat treatments on optical properties such as translucency and color duplication does not have a cutting end in the literature up to the authors' knowledge [6,30,31]. This study simulates two of the third-level thermal tempering protocols in the laboratory and explores their impact on aesthetic parameters such as the color and translucency of four lithia-silicate pressed glass ceramics, providing recommendations for the clinical implications of such tempering protocols regarding esthetics. The null hypothesis was that no significant difference in optical properties between two lithia-silicate and two lithia-zirconia silicate pressable glass ceramics tested and that the thermal tempering procedures had no significant impact on these properties.

MATERIAL AND METHODS

Sample preparation

Out of 40 pressable lithia-silicate ceramic ingots, 40 rounded discs measuring 15 mm in diameter and 1 mm in thickness were created. These discs were then categorized into 4 groups (n=10) according to the composition of the material used;

Two lithia-silicate glass ceramics (LSGCs) used in this study were:

- Gp (E) (IPS e.max Press; Ivoclar Vivadent AG),
- Gp (L) (GC Initial LiSi Press, GC).

While the two Lithia-zirconia silicate (LZSCs) glass ceramics used in this study were:

- Gp (C) (Celtra Press, Dentsply Sirona) and
- Gp (A) (VITA Ambria, VITA Zahnfabrik).

For construction of these samples, Wax patterns (Elastiwax; Keram & Keramik) were made in a special Teflon mold with the desired geometry, sprued and invested (IPS e.max Special Investment Material; Ivoclar Vivadent AG), the wax eliminated at 850 °C for 1 hour, and the ingots were pressed in a furnace (EP600; Ivoclar Vivadent AG) as per the protocol recommended by each manufacturer as shown in Table I.

The specimens were divested by sandblasting with 50 μm alumina particles at 4 bars of atmospheric pressure. Then smooth divesting was used at 2 bars till complete removal of investment material from discs. After sprues were separated by separating diamond discs, each attachment point was smoothened by a diamond disc. The samples were finally finished and polished using (Optrafine Ceramic Polishing System) sequentially, using the first tip for 60 seconds with a speed of 10000 rpm. While the next tip was used for the same duration

Table I - Recommended pressing temperatures of ceramics

Group	(T0)
Gp (A)	880 °C
Gp (C)	870 °C
Gp (E)	917 °C
Gp (L)	910 °C

of 60 seconds, but with a slower speed of 6000 rpm to simulate the clinical situation.

First phase measurements

Optical properties measurements

The color was measured on both a black and white background using Aglient Cary 5000 UV-Vis-NIR spectrophotometer (Agilent Technologies, Santa Clara, USA) where the discs were aligned in the device that is considered a PC and a spectrophotometer unit. The light beam passes from the tungsten lamp through a double monochromator to allow being monochromatic. Then passes through the sample to the detector. The passing light beam is detected by a photomultiplier that is sensitive to ultraviolet regions. The wavelength ranged from 380 to 780 nm. CIE L*a*b* color values for each sample were then calculated from the diffuse reflectance using color software which is available through the Cary WinUV instrument and supports extensive color standards and calculations.

L^* Is a measure of the lightness-darkness of material (perfect black has an $L^* = 0$, and perfect white has an $L^* = 100$).

The a^* coordinate is a measure of the redness (positive value) or the greenness (negative value), while the b^* coordinate is a measure of the yellowness (positive value), or the blueness (negative value).

The translucency parameter (TP) was obtained by calculating the color difference between specimens over black and white backgrounds.

$$TP = \left[(Lb - Lw)2 + (ab - aw)2 + (bb - bw)2\right]½ \quad (1)$$

where: (b) refers to color coordinated over a black background; (w) refers to color coordinated over a white background.

While Contrast ratio (CR) was calculated through;

$$CR = YB/YW \quad (2)$$

$$Y = \left(\left[½L+16\right]–116\right)^3 \times 100 \quad (3)$$

And the CR range was defined from 0 (transparent) to 1 (totally opaque).

Scanning electron microscope (SEM)

A Field Emission Scanning Electron Microscope (FESEM, Carl Zeiss Ultra, Oberkochen, Germany) was used to analyze the microstructure. The glass-ceramics microstructure was examined using the specimens. Using an etched specimen, the crystallite microstructure was investigated. The specimens were cleaned with distilled water and then etched for 20 seconds using a 9.5% hydrofluoric acid gel. The operating distance was 8 mm, and the acceleration voltage was 5 kV. Before SEM examination, all specimens were gold sputter-coated to avoid charging effects during imaging.

X-ray diffraction analysis

Bruker's AXS D8 Advance X-ray diffractometer was used to examine the samples' mineralogy using monochromatic Cu K α x-ray angle (= 1.5406 Å). With a counting time of two seconds per step and a step size of 0.006◦(2), X-ray diffractograms were obtained between 10◦ and 60◦(2). ICSD reference data served as the basis for phase identification.

Energy dispersive X-ray analysis (EDX)

A non-destructive X-ray technology termed energy dispersive X-ray analysis (EDX) was implemented to figure out the elemental makeup of materials. The specimen of interest was identified by the microscope imaging on Electron Microscopy instruments, which have been equipped with EDX systems. The obtained EDX findings are provided as spectra that display the peaks of the analysis's compositional constituents.

Thermal tempering

Following that, each major group of the four LSCs was split into two groups (n = 5) in accordance with the thermal tempering procedure, as follows:

- Sub gp T1 (n = 10), where specimens were fired at a temperature 9% below the pressing temperature;
- Sub gp T2 (n = 10) the specimens underwent a firing cycle at a temperature 5% below the pressing temperature based on the following fire charts for each material.Recommended tempering temperatures are shown in Table II.

Second phase measurements

Optical properties measurements, Scanning Electron Microscopic analysis (SEM), X-ray Diffraction analysis (XRD), and Energy Dispersive X-ray Analysis (EDX) were repeated for all samples after thermal tempering the same way discussed earlier.

Statistical analysis

Using tests of normality (Kolmogorov-Smirnov and Shapiro-Wilk tests) and examining the data distribution, numerical data were examined in preparation for statistical analysis. The data were all parametrically distributed. The mean and standard deviation (SD) values of the data were displayed. Two-way ANOVA testing and repeated measures ANOVA were employed. When the ANOVA test was significant, pairwise comparisons were performed using Bonferroni's post-hoc test.

RESULTS

Translucency: at T0 Pairwise comparisons between LSCs types revealed there was a statistically significant difference between them (*P*-value <0.001, Effect size = 0.998). that Gp (E) showed the statistically significantly highest mean TP. Gp (L) showed a statistically significantly lower mean TP followed by Gp (A) with a statistically significant difference between the two ceramics. Gp (C) showed the statistically significantly lowest mean as shown in Table III.

After heat treatment whether with T1 or T2, in all groups and subgroups, there was a statistically significant increase in mean TP after thermal tempering. Comparing the two tempering protocols, T1 showed statistically significantly lower TP mean values than T2. The difference was significantly highest recorded for Gp (E).

In terms of CR mean values, the results showed that LSCs type had a statistically significant effect on mean CR (*P*-value <0.001, Effect size = 0.995). recorded the significantly highest CR mean values for (LZSC) in Gp (C) and Gp (A), followed by Gp (L) and Gp (E) respectively. The selected thermal tempering whether T1 or T2 had a statistically significant decrease in mean CR (*P*-value <0.001, Effect size = 0.96). while the effect of changing the temperature of the thermal tempering procedure had no statistically significant effect on mean CR (*P*-value = 0.694, Effect size = 0.005).

Table II - Recommended tempering temperatures of ceramics

Group	(T0)	(T1)	(T2)
Gp (A)	880 °C	800 °C	836 °C
Gp (C)	870 °C	790 °C	826 °C
Gp (E)	917 °C	835 °C	872 °C
Gp (L)	910 °C	828 °C	865 °C

Color changes

Table IV shown a significant shift in color in all groups witnessed after the selected thermal tempering procedures, being highest evidenced in Gp (E) with ΔE values of (3.18± 0.2) followed by Gp (L) ΔE of (2.47± 0.19) then Gp (C) ΔE of (2.26 ±0.14) and the last Gp (A) ΔE (1.62 ±0.13).

The T2 thermal tempering procedure provided a noticeably greater color shift ΔE mean value of (2.55 ± 0.63) against ΔE of (2.35 ± 0.59) with the T1 protocol.

With thermal tempering, the shift was caused by an increase in L* parameter values and moving positively toward redness in a* parameter consistently with moving toward the yellow direction in b* as shown in Table V.

Scanning electron microscopy

Typically, Gp (ET0) showed multilayered crystals in the form of rods lying parallel to the direction of pressing with the average crystal's length × width diameters of 3 μm × 680 nm (Figure 1A). For Gp (ET1), the length and width grew to 4.5 μm and 700 nm, respectively (Figure 1B). Further growth to 4 μm length and 870 nm width with Gp (ET2) (Figure 1C).

Table III - The mean, standard deviation (SD) values and results of repeated measures ANOVA test for comparison between TP of ceramic types

Gp (E)		Gp (L)		Gp (A)		Gp (C)		*P*-value	Effect size *(Partial eta squared)*
Mean	SD	Mean	SD	Mean	SD	Mean	SD		
17.53^{A}	0.89	15.5^{B}	0.7	13.69^{C}	0.54	12.24^{D}	0.4	<0.001*	0.998

Table IV - The mean, standard deviation (SD) values and results of the two-way ANOVA test for comparison between ΔE of ceramic types regardless of temperature

Gp (E)		Gp (L)		Gp (C)		Gp (A)		*P*-value	Effect size *(Partial eta squared)*
Mean	SD	Mean	SD	Mean	SD	Mean	SD		
3.18 [A]	0.2	2.74 [B]	0.19	2.26 [C]	0.14	1.62 [D]	0.13	<0.001*	0.957

*: Significant at P ≤ 0.05

Table V - Average change values of L* a* b* after heat treatments

		ΔL	Δa	Δb	ΔE
Gp E	T1	1.47	1.17	2.40	3.05
	T2	1.56	1.40	2.55	3.30
Gp L	T1	1.26	1.10	2.02	2.63
	T2	1.40	1.09	2.23	2.85
Gp C	T1	1.20	0.67	1.69	2.18
	T2	1.28	0.84	1.76	2.34
Gp A	T1	0.92	0.67	1.04	1.55
	T2	1.02	0.70	1.14	1.69

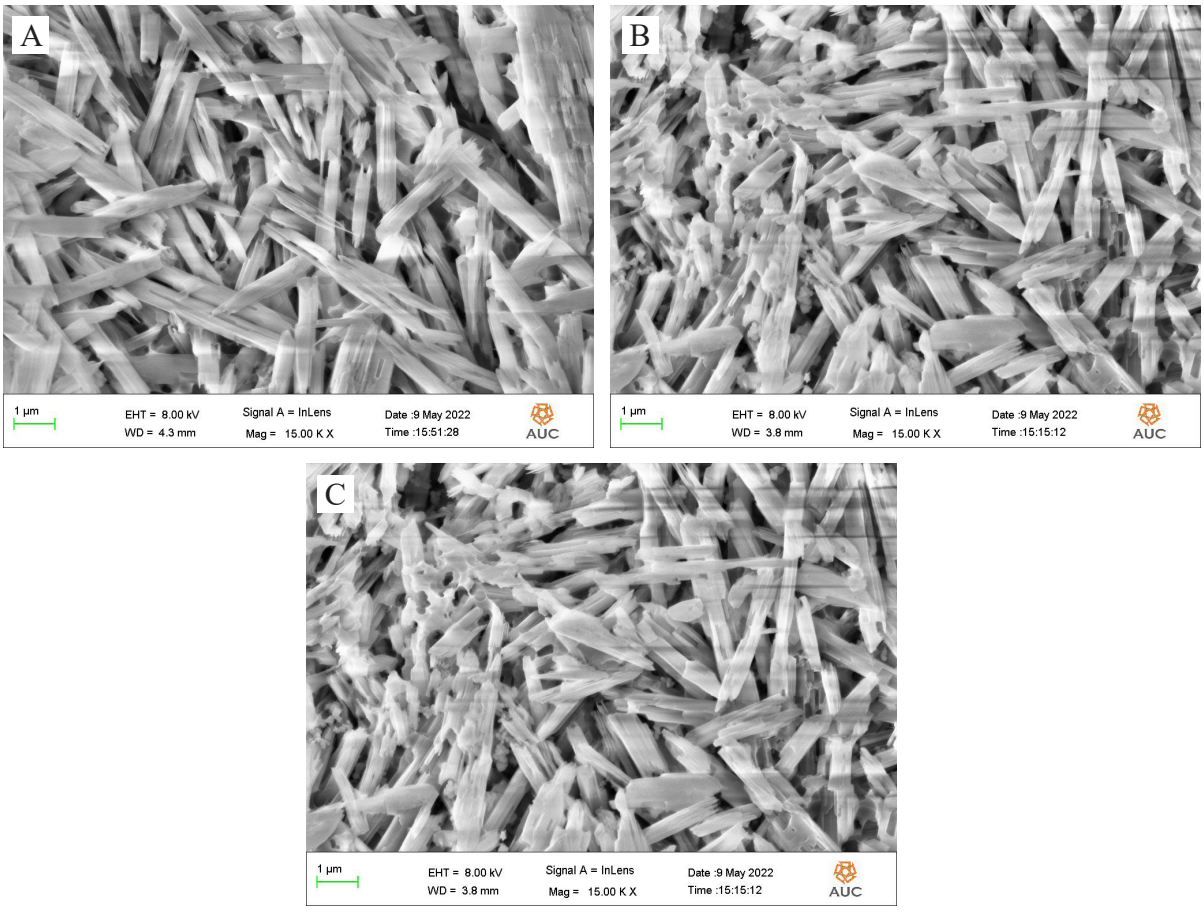

Figure 1 - (A) SEM IPS e.max Press without tempering; (B) SEM showing IPS e.max Press after the first heat tempering at 9%; (C) SEM showing IPS e.max Press after the second heat tempering at 5%.

Comparing the Gp (LT0) group to the Gp (ET0) group, there is a noticeable difference in the microstructure; An interlocking microstructure was formed by layering platelet-shaped crystals embedded in the glass matrix. The crystals were not oriented parallel to the direction of pressing as compared to Gp (ET0). The crystals in the Gp (LT0) featured an average length of 2 um and a diameter of 600 nm (Figure 2A). In contrast, Gp (LT1) (Figure 2B) displayed 2.5 um in length

and 630 nm in width. Meanwhile, reaching a length of 2.4 um and 985 nm width with Gp (LT2) (Figure 2C).

The microstructure of Gp (CT0) was found to be interlocking, with an average crystal length of 1.8 um and a width of 500 nm (Figure 3A). The crystal's length shrank to 1.3 um and its width expanded to 600 nm in Gp (CT1) (Figure 3B). The length increased to 2 um as well as its width significantly increased to 770 nm in the (GpC) T2 (Figure 3C).

Figure 4A of Gp (AT0) revealed needle-like crystals with an average length of 3 um and a width of 380 nm. Figure 4B of Gp (AT1) revealed an additional increase in the length and width of the crystals, measuring 4.5 um and 530 nm, respectively. The lithium disilicate crystals in Gp (AT2) solidified and shrank in size (Figure 4C), which made it challenging to estimate grain sizes with any degree of accuracy.

X-ray diffraction

Major peaks of lithium disilicate ($Li_sSi_2O_5$) were observed at 2θ values of 24.7°, and 40 degrees. Traces of lithium phosphate (Li_3PO_4) were detected in all groups while traces of Lithium metasilicate (Li_2SiO_3) traces were detected with Gp (C) and Gp (A). The dominant peak (highest peak) was at 24.7 degrees. The XRD data showed the highest peak intensity in Gp (E) equally in T0, T1, and T2, while for Gp (L) highest peak intensity was at T1 with equal intensities in T0 and T2. For Gp (C) the highest peak is with T2 and the least was with T0. For Gp (A) the highest intensity was at T0 and the lowest intensity at T1 (Figures 5, 6, 7 and 8).

Energy dispersive X-ray analysis (EDAX)

Minor differences in compositions between materials and thermal tempering protocols were analyzed as shown in the Figures 9, 10, 11 and 12 below.

DISCUSSION

The study aimed to assess how specific thermal tempering techniques affect the optical characteristics of pressable LSCs whether with LSGCs or LZSCs. The selection of those specific two thermal protocols was based on the 'manufacturer's recommendation of one

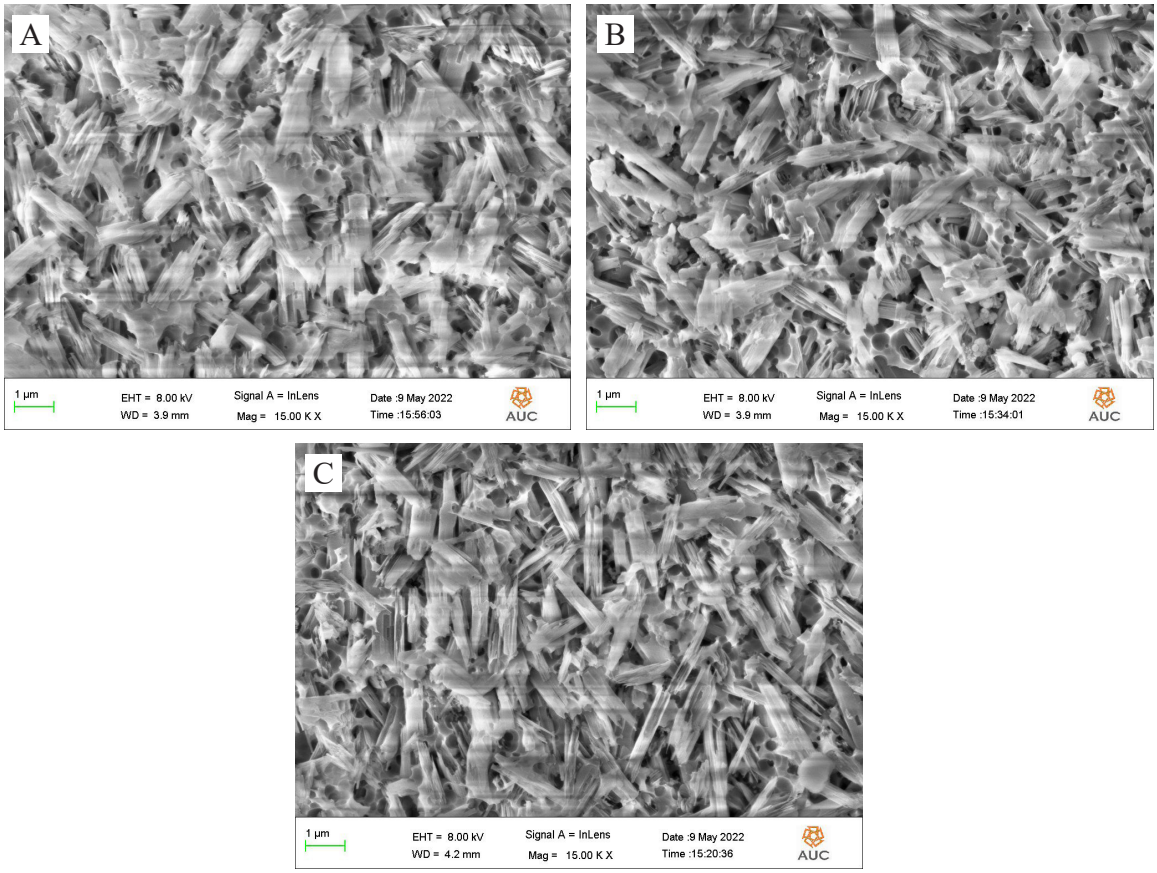

Figure 2. (A) SEM GC Initial LiSi Press without tempering); (B) SEM showing GC Initial LiSi Press after the second heat tempering at 9%; (C) SEM showing GC Initial LiSi Press after the second heat tempering at 5%.

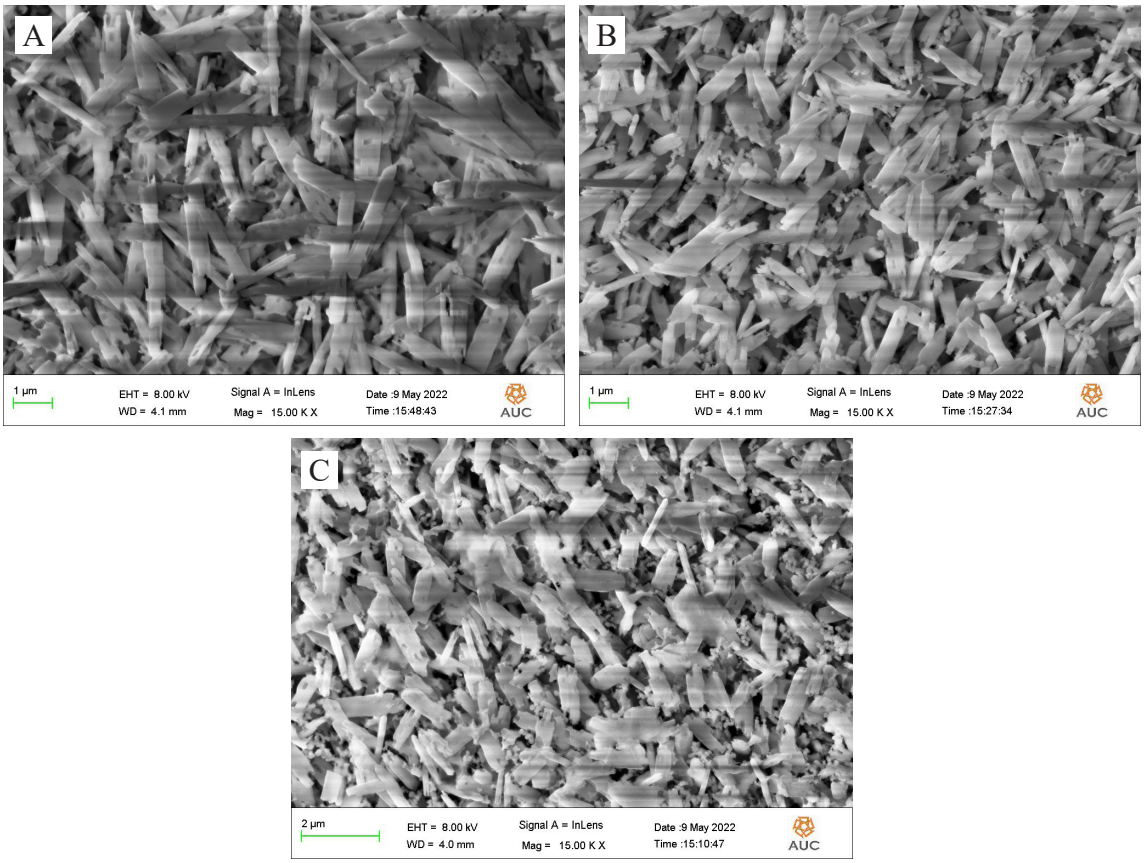

Figure 3 - (A) SEM Celtra Press without tempering; (B) SEM showing Celtra Press after the second heat tempering at 9%; (C) SEM showing Celtra Press after the second heat tempering at 5%.

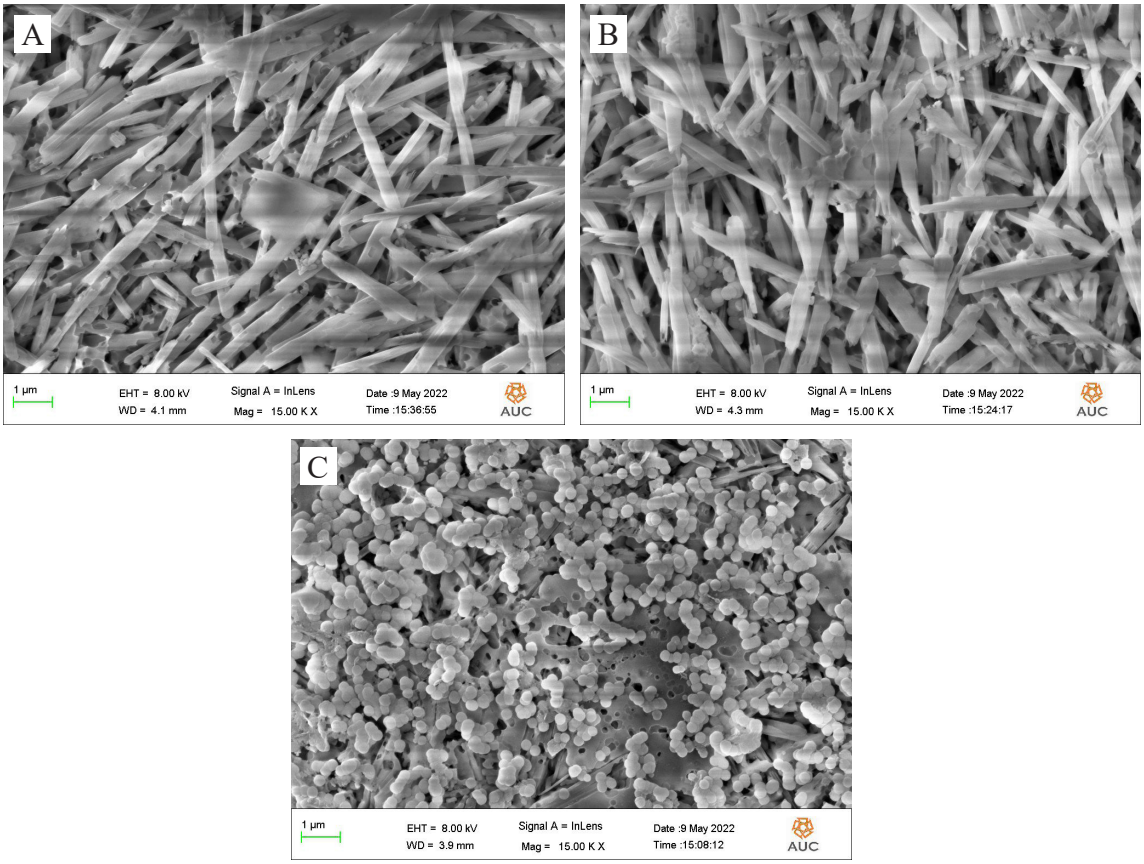

Figure 4 - (A) SEM VITA Ambria Press without tempering; (B) SEM showing VITA Ambria Press after the second heat tempering at 9%; (C) SEM showing VITA Ambria Press after the second heat tempering at 5%.

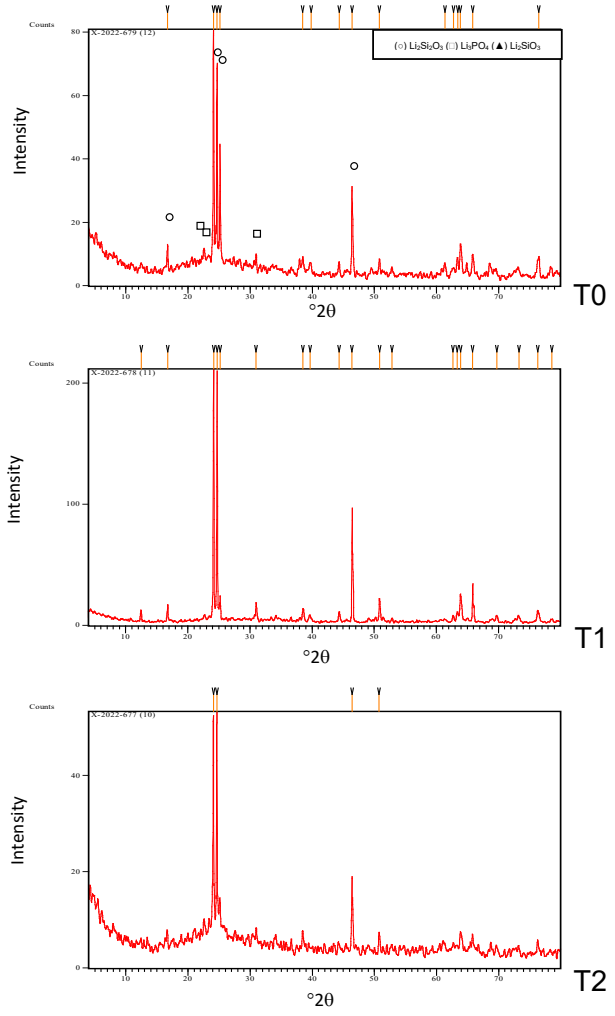

Figure 5 - XRD analysis of IPS E.max Press, (T0) control group, (T1) tempering at 9% below pressing temperature, and (T2) tempering at 5% below pressing temperature.

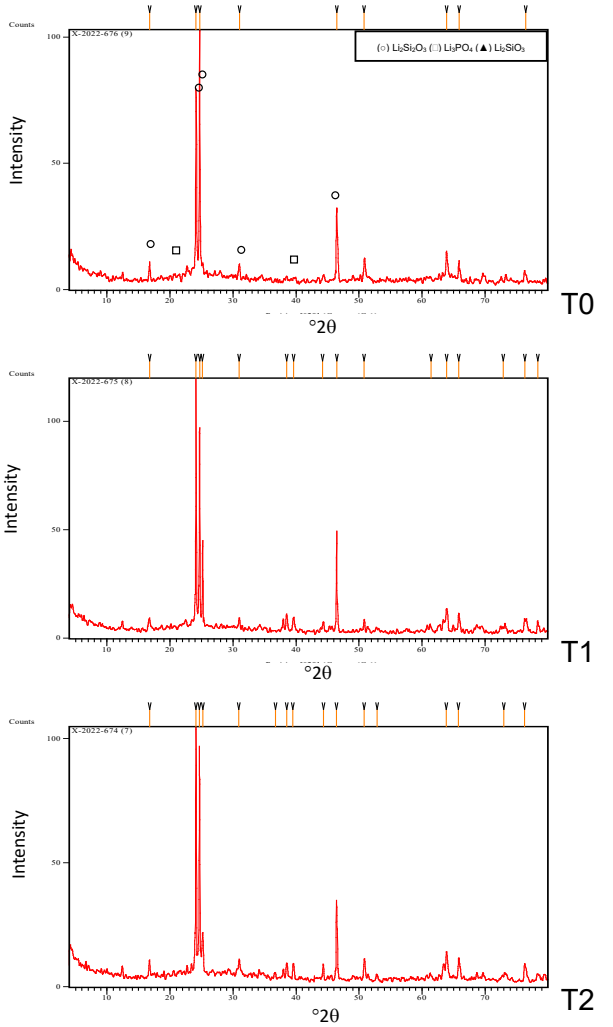

Figure 6 - XRD analysis of LiSi Press (T0) control group, (T1) tempering at 9% below pressing temperature and (T2) tempering at 5% below pressing temperature

of the selected materials for an additional firing cycle at a temperature of 9% below the pressing temperature [29]. The second protocol was selected with 5% below the pressing temperature which is the maximum limit for temperature deviations below the pressing and should not be exceeded by any means [32,33]. The obtained results demonstrated that the chosen thermal tempering processes could have a considerable impact on the optical result of these chosen materials, rejecting the null hypothesis. Translucency is a vital key optical property that can be employed to replicate the appearance of natural teeth and precisely match with the surrounding structure, particularly in the anterior and esthetic zones [34]. The translucency of lithium disilicate glass-ceramics depends on several factors such as: thermal history, pressure, time (for heat-pressed), amount and type of nucleating agent, crystal morphology, microstructure, glass matrix, volume ratio crystal/glass and difference in the refractive index between these phases, phase composition and chemical composition including grain boundaries, pores, second-phase component, additives, and light scattering from the surface [35].

Effect on translucency

Before any thermal process: at T0

The translucency was greatly impacted by the type of LSCs utilized, as seen by the TP mean values. The LSCs recorded significantly higher translucency than the LZSCs as; Gp (E) recorded the significantly highest mean TP value (TP=17.52), according to published literature [36], this is within the same translucency range of 1 mm for human enamel and dentin, which are 18.7 and 16.4, respectively. This implies this material is best suited as an aesthetic material for anterior cases. Gp(L), with a mean

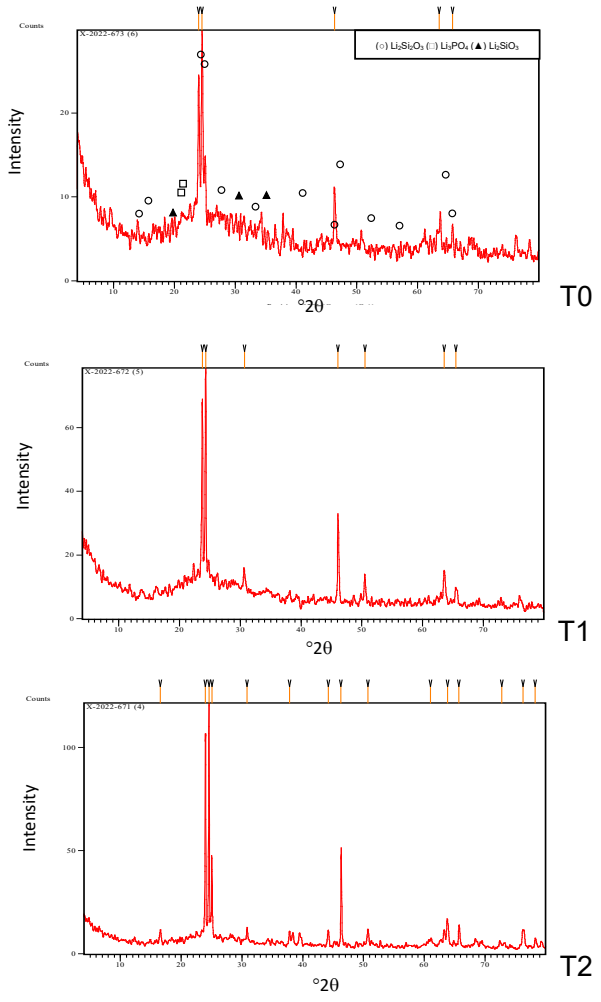

Figure 7 - XRD analysis of Celtra Press, (T0) control group, (T1) tempering at 9% below pressing temperature, and (T2) tempering at 5% below pressing temperature.

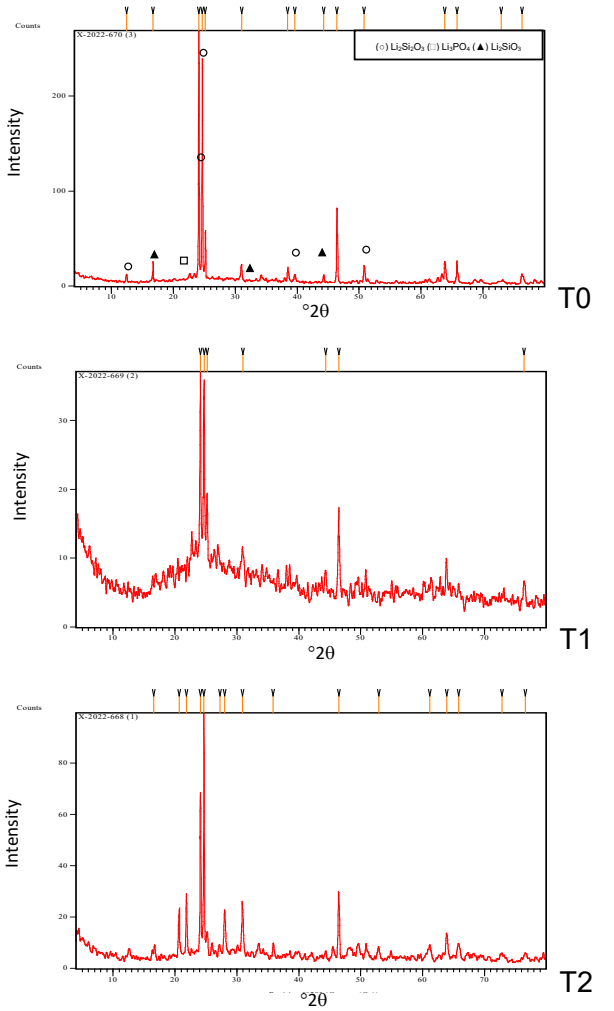

Figure 8 - XRD analysis of VITA ambria, (T0) Control group, (T1) tempering at 9% below pressing temperature, and (T2) Tempering at 5% below pressing temperature

TP value of (TP=15.5), came next. Even though both materials have considerable crystallinity, the matching of refractive indices between their crystalline phase 1.55 and glassy phase 1.50, which permits greater light transmission, was considered one of the main causes for their unique translucency [37].

Since it has been shown that lithium disilicate crystals obstruct light transmission, varying the size of the crystals in these materials can result in varying levels of translucency. An earlier investigation comparing the translucencies of IPS e.max CAD LT, MT, and HT concluded that the larger crystal sizes of the IPS e.max HT reduced its dispersion and lowered its crystal density, which in turn led to its higher translucency [38]. SEM analysis showed that GP (E) has larger rod-shaped crystals with an average measured length of 2.762-3.293 μm and an average measured width of 533.5-687.9 nm, while GP (L) has more rounded smaller platelet-shaped crystals with an average measured length of 2.2μm and an average width of 580nm. Similar crystal sizes for both materials were reported by Ohashi et al. [39]. Further differences in spatial crystal arrangement were revealed by the SEM analysis. For example, the crystals in Gp (E) aligned parallel to the sample surface in an interlocking arrangement, indicating the pressing direction. Conversely, the scanning image of GP (L) revealed platelet-shaped crystals that were randomly oriented, densely fused and had a highly interlocking microstructure with irregular edges. In contrast to (Gp E), the crystals' orientation was not parallel to the pressing plane. Higher transmittance values may be explained by the linear, more ordered crystalline structure, whereas the noticeably lower transmittance values for the Gp (L) may be explained by the irregular crystal arrangement, which increases scattering and reflectance in addition to increasing the incidence of porosities, which negatively affects translucency due to the mismatch between the

Group (E):

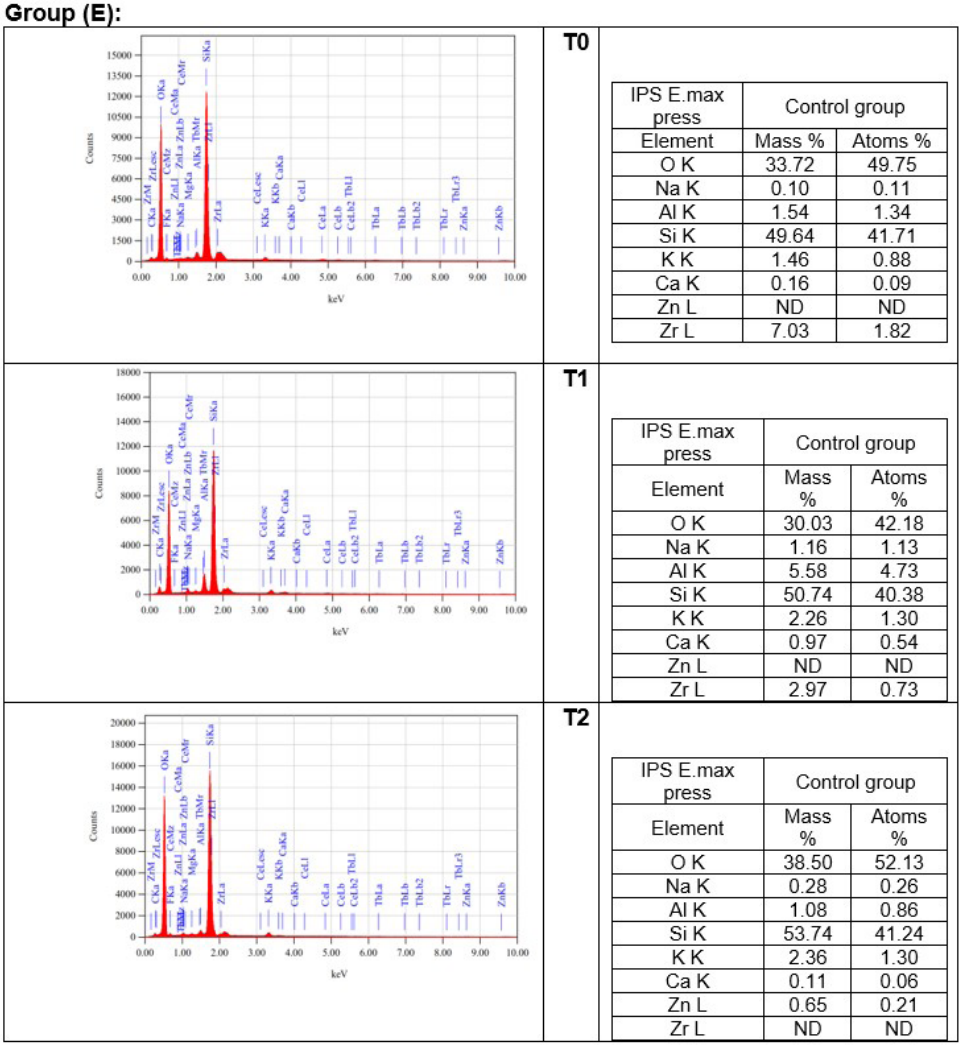

IPS E.max press	Control group	
Element	Mass %	Atoms %
O K	33.72	49.75
Na K	0.10	0.11
Al K	1.54	1.34
Si K	49.64	41.71
K K	1.46	0.88
Ca K	0.16	0.09
Zn L	ND	ND
Zr L	7.03	1.82

IPS E.max press	Control group	
Element	Mass %	Atoms %
O K	30.03	42.18
Na K	1.16	1.13
Al K	5.58	4.73
Si K	50.74	40.38
K K	2.26	1.30
Ca K	0.97	0.54
Zn L	ND	ND
Zr L	2.97	0.73

IPS E.max press	Control group	
Element	Mass %	Atoms %
O K	38.50	52.13
Na K	0.28	0.26
Al K	1.08	0.86
Si K	53.74	41.24
K K	2.36	1.30
Ca K	0.11	0.06
Zn L	0.65	0.21
Zr L	ND	ND

Figure 9 - Microanalysis by EDAX of Gp(E), (T0) Control group, (T1) tempering 9% below pressing temperature and (T2) tempering 5% below pressing temperature.

air refractive index and the other phases. Similar microstructural observations were found when Hallman et al. [35] investigated the microstructure of the same materials following pressing.

The pressing temperature for both ceramics was above 900 °C where a complete transformation to lithium disilicate $Li_2Si_2O_5$ occurred with only minor traces of lithium orthophosphate Li_3PO_4. This was evident with the XRD analysis at T0.

In terms of the lowest TP mean values for the LSCs; the two LZSCs were ordered as follows; GP (A) and Gp (C) (TP = 13.69 and 12.24, respectively). As mentioned by Yan et al. [40], the 8-12% zirconia content in these materials may seem to be the cause of the increased dispersion and decreased transmission. This reason could not be fully depended upon in our investigation because hardly any phases containing zirconia were found, either in XRD or in EDAX analysis, which outweighed the dissolution during the crystallization procedure. The Zr role was evident in modifying the crystallization process and increasing the viscosity of the glassy matrix. It proved that the presence of ZrO and AlO allowed the precipitation and domination of the lithium metasilicate Li_2SiO_3 phase at a temperature of around 700 °C as stated by Zhang et al. [15], which is then reacted again, at higher temperatures of pressing at 880-870 °C, with the silica in the glass matrix to form the lithium disilicate crystal phase. This final reaction was not complete with both LZSCs tested materials as traces of the lithium metasilicate phase were evident in XRD analysis at T0. This is logically one of the reasons for hindering the translucency of these materials. Besides the smaller crystal sizes were evident through SEM analysis as the crystals were narrower and more irregularly arranged.

Group (L):

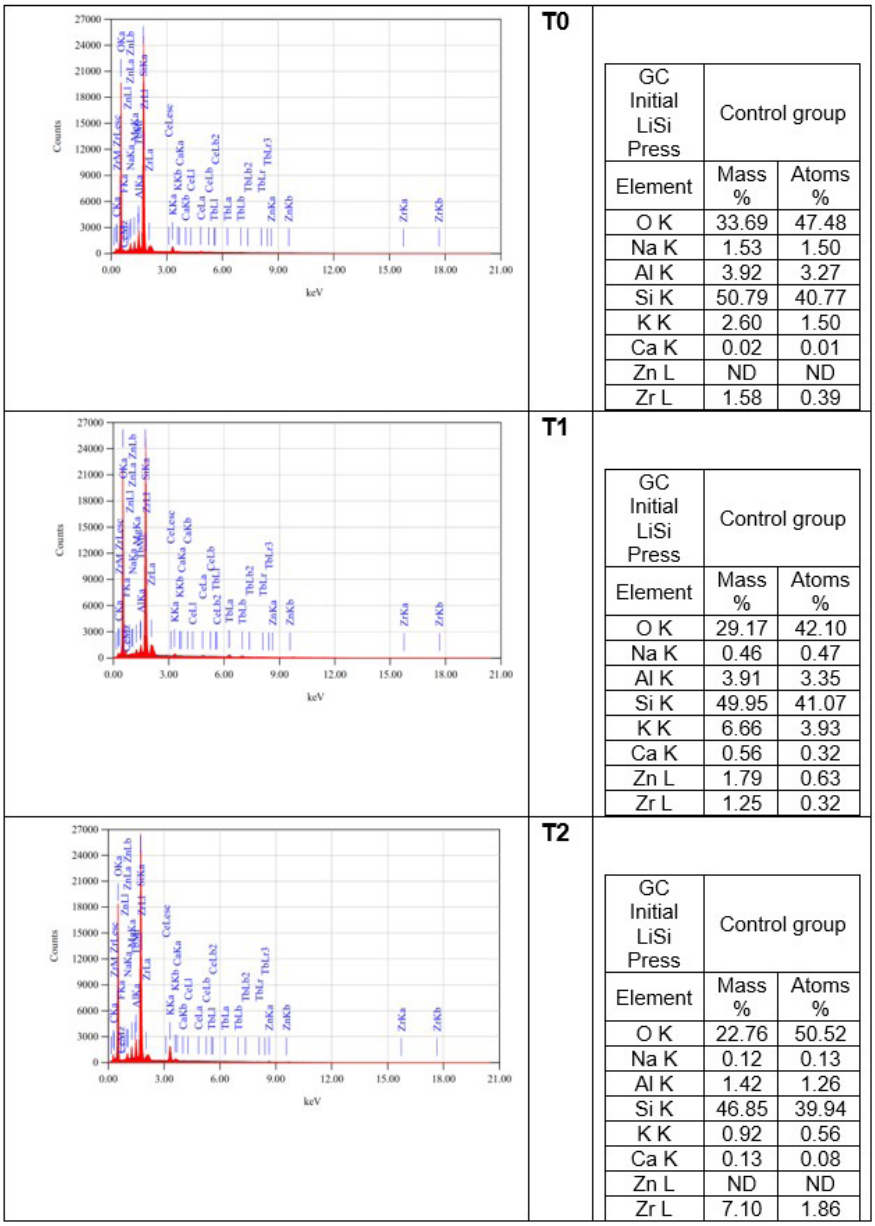

GC Initial LiSi Press	Control group	
Element	Mass %	Atoms %
O K	33.69	47.48
Na K	1.53	1.50
Al K	3.92	3.27
Si K	50.79	40.77
K K	2.60	1.50
Ca K	0.02	0.01
Zn L	ND	ND
Zr L	1.58	0.39

GC Initial LiSi Press	Control group	
Element	Mass %	Atoms %
O K	29.17	42.10
Na K	0.46	0.47
Al K	3.91	3.35
Si K	49.95	41.07
K K	6.66	3.93
Ca K	0.56	0.32
Zn L	1.79	0.63
Zr L	1.25	0.32

GC Initial LiSi Press	Control group	
Element	Mass %	Atoms %
O K	22.76	50.52
Na K	0.12	0.13
Al K	1.42	1.26
Si K	46.85	39.94
K K	0.92	0.56
Ca K	0.13	0.08
Zn L	ND	ND
Zr L	7.10	1.86

Figure 10 - Microanalysis by EDAX of Gp(L), (A) Control group, (B) tempering 9% below pressing temperature, and (C) tempering 9% below pressing temperature.

Consistently the significantly highest CR mean value was for LZSCs: GP (C) followed by GP (A) with no significant difference between them, and then the two other groups of LSCs; Gp (L) and GP (E) the significantly lowest. The non-significance between both LZSCs groups may be attributed to that the CR is mainly for measuring opacity and small light transmittance differences can't be detected through such measurement, while TP is calculated through the color parameters that give a more accurate indication about the light transmittance.

Effect of thermal tempering on translucency

Regardless of the ceramic type and temperature of the tempering process there was a significant increase in translucency with thermal tempering expressed in a considerable increase in TP mean value paralleled with a significant decrease in CR values. This is consistent with Farahnaz Nejatidanesh et al. [41] study results that a significant increase in translucency with repeated firing was reported. This might be explained by the fact that heat treatment causes the crystals to grow larger while also changing

Group (C):

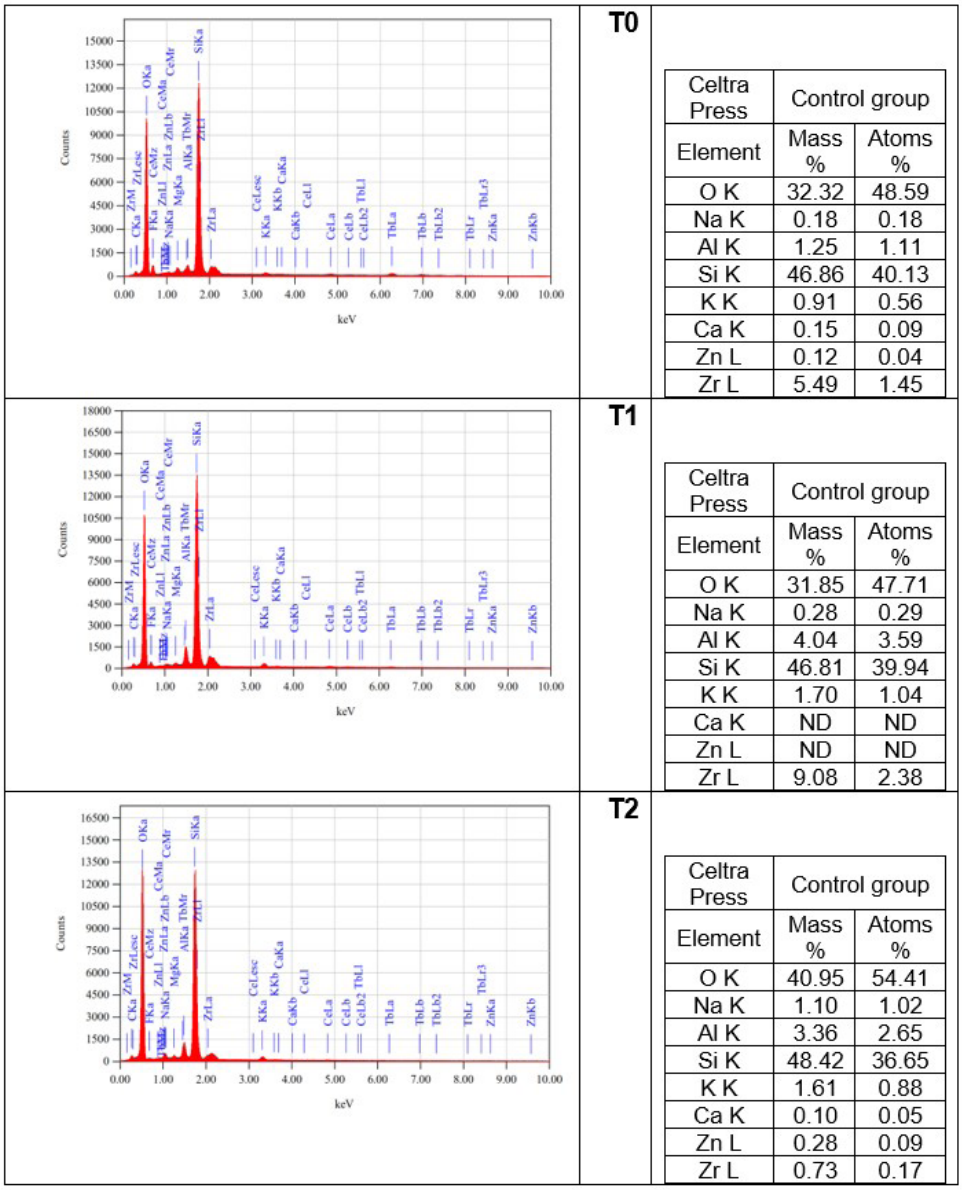

Celtra Press	Control group	
Element	Mass %	Atoms %
O K	32.32	48.59
Na K	0.18	0.18
Al K	1.25	1.11
Si K	46.86	40.13
K K	0.91	0.56
Ca K	0.15	0.09
Zn L	0.12	0.04
Zr L	5.49	1.45

Celtra Press	Control group	
Element	Mass %	Atoms %
O K	31.85	47.71
Na K	0.28	0.29
Al K	4.04	3.59
Si K	46.81	39.94
K K	1.70	1.04
Ca K	ND	ND
Zn L	ND	ND
Zr L	9.08	2.38

Celtra Press	Control group	
Element	Mass %	Atoms %
O K	40.95	54.41
Na K	1.10	1.02
Al K	3.36	2.65
Si K	48.42	36.65
K K	1.61	0.88
Ca K	0.10	0.05
Zn L	0.28	0.09
Zr L	0.73	0.17

Figure 11 - Microanalysis by EDAX of Gp(C), (T0) Control group, (T1) tempering 9% below pressing temperature and (T2) tempering 5% below pressing temperature.

the pore size, crystal distribution, and crystal orientation. The growth of crystals followed distinct axes based on the nature of ceramic and microstructure, leading to a phenomenon known as "*Ostwald ripening*" in published works [35], where tiny crystals are sacrificed in favor of bigger ones. This was evident by the SEM analysis that revealed an increase in length and width measurements of crystal size after thermal tempering. For the non-zirconia reinforced LGSCs, these were considered the main reasons for increasing translucency. While for the other two LZSCs Gp (A) (T1, T2) and Gp (C) (T1, T2) we could include the reason for further crystallization of the remaining glass matrix. The pressing temperature for these two types was lower than that of the others which might have caused incomplete maturation of lithium metasilicate crystals as mentioned before concerning XRD analysis. Subjecting these materials to a second hit of thermal treatment at a temperature somewhat lower than their pressing temperature provided the opportunity for full, as evidenced by higher peaks of $LI_2SI_2O_5$ in XRD.

Comparing the tempering temperature T1 and T2, in terms of TP mean values, Our research's findings indicated that selecting a

Group (A):

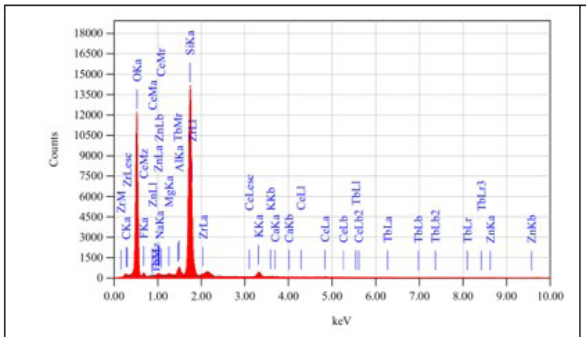

VITA Ambria	Control group	
Element	Mass %	Atoms %
O K	38.37	52.05
Na K	0.20	0.19
Al K	1.85	1.49
Si K	52.46	40.53
K K	2.54	1.41
Ca K	0.21	0.12
Zn L	0.40	0.13
Zr L	0.20	0.05

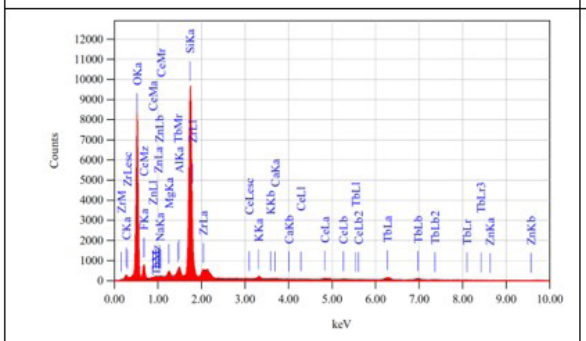

VITA Ambria	Control group	
Element	Mass %	Atoms %
O K	30.03	42.18
Na K	1.16	1.13
Al K	5.68	4.73
Si K	50.47	40.38
K K	2.26	1.30
Ca K	0.97	0.54
Zn L	ND	ND
Zr L	2.97	0.73

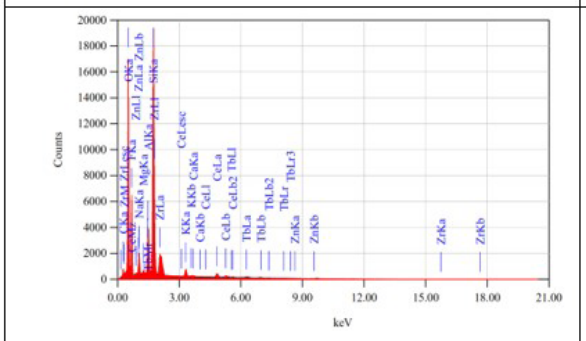

VITA Ambria	Control group	
Element	Mass %	Atoms %
O K	38.70	52.13
Na K	0.28	0.26
Al K	1.08	0.86
Si K	53.74	41.24
K K	2.36	1.20
Ca K	0.11	0.06
Zn L	0.65	0.21
Zr L	ND	ND

Figure 12 - Microanalysis by EDAX of Gp(A), (T0) Control group, (T1) tempering 9% below pressing temperature and (T2) tempering 5% below pressing temperature.

tempering temperature T2 of 5% below the pressing temperature T0 would significantly boost the translucency of LSCs compared to T1 of 9% below the pressing temperature T0. GP (E) was the greatest expression of it. This was about the same heat-treated microstructural and compositional modifications that were previously discussed. It makes sense for these changes to be more pronounced at higher temperatures that are closer to pressing, as shown by the T2 groups. While in terms of CR values the decrease in opacity recorded was statistically insignificant in all groups for both tempering protocols. This was related to the nature of the CR parameter as mentioned before.

Change in color parameters

The glass-ceramics utilized in this investigation had the same translucency (medium, MT) and color (A2), per manufacturer data. All Groups showed a significant shift in color after thermal tempering regardless of tempering temperature, being ordered from the most stable material with minimal ΔE of 1.62 (just above the Perceptibility thresholds) that was GP (A), followed by GP (C) of ΔE=2.26, then GP Lisi of ΔE= 2.44 and the greatest shift in color was with GP (E) with ΔE= 3.18. Thresholds for acceptability and perceptibility were established

based on information from published literature on these values [42].

For the temperature effect, the T1 group expressed significantly less shift in ΔE than Group T2 both being in the range of acceptability. The formation of a new crystal phase, or the size change of the original crystal, the disappearance of impurities and other low-melting substances, resulting in the fusion of the main crystal phase and the change of the ceramic surface structure. Thus, the color changes accordingly. It had been found that this color shift was attributed to the shift in all the color parameters. An increase in L* values of color parameters which means an increase in the brightness of the material [43], was recorded with an average increase of ΔL=1.25 being mostly expressed in Gp (ET2) with ΔL=1.47 and least in Gp (AT1) with ΔL= 0.9. This was not expected consistently with the increase in translucency that implies usually increase in the amount of transmission. A previous study by Dong-Dong et al. [44] pointed out a total downward L* value with repeated sintering however in the same work they pointed out an initial increase in value level with the first three additional sintering cycles which was then decreased with the increase in number of sintering cycles. So it is consistent with our results as we added a single tempering cycle with different temperatures in each subgroup (T1 & T2). According to the pre-discussed microstructural changes with heat application, crystal size at growth at the expense of the glassy phase volume and the pores size and distributional changes lead to increased translucency. A combination of reducing the porosity and decreasing boundaries and interfaces may have caused an increase in the homogeneity of its crystalline structure, which promoted higher specular reflectance and optical transmission with minimized refraction and absorption, this may have been due to the grain and pore distribution volume reduction, this new scattering pattern increased in specular reflectance elevating the L* value yet allowing more transmission. The highest value indicating the largest shift in color parameters was with Δb values toward the yellow direction with maximum value for Gp (ET2) Δb = 2.55 and lowest with Gp (AT1) Δb= 1.04. The metallic pigment particles infused in the parent ceramic formula are primarily responsible for the variation in chroma [45]. By incorporating various kinds and concentrations of pigment particles, ceramic materials may exhibit a range of hues. Typically, pigments are made of metal oxides that can withstand high temperatures, such as manganese oxides, zinc, iron red, chromium red, and titanium yellow [46]. The pigment's chemical structure may alter as a result of thermal tempering, changing the hue [47]. Furthermore, the dissolution or melting of pigment particles upon tempering may alter the ceramic's hue as well as how the particles react to incident light. The shift toward redness was the least among all color parameters being most recorded to GP (ET2), Δa= 1.40, and least equal with GP (CT1) and Gp (AT1), Δa=0.67, in all cases, the most shift in color was recorded to non-reinforced LGSCs, with IPS emax being the highest affected specially with T2 tempering protocol where the temperature was 5% lower than the pressing temperature, while for zirconia reinforced LZSCs color shift was minimal being least apparent with Vita Ambria at T1 tempering temperature.

CONCLUSION

Within the limitations of the present study, the following conclusions could be made:

1) The most translucent lithium disilicate types (E. Max Press – LiSi Press) are the most susceptible to change in color and translucency with exposure to thermal tempering protocols;
2) Zr-reinforced lithium silicate-based ceramics are less sensitive to optical changes with additional heat treatments;
3) Increasing the tempering temperature near the pressing temperature had a greater positive impact on the color and translucency of pressable lithium disilicates.

Author's Contributions

IHEA: Formal Analysis, Investigation, Writing – Review & Editing. AEE: Conceptualization, Methodology, Data Curation. SMF: Writing – Original Draft Preparation, Supervision.

Conflict of Interest

The authors have no conflict of interest.

Funding

The authors have no funding for this article.

Regulatory Statement

The authors have no proprietary, financial, or other personal interest of any nature or kind in any product, service, and/or company that is presented in this article.

REFERENCES

1. van den Breemer CR, Vinkenborg C, van Pelt H, Edelhoff D, Cune MS. The clinical performance of monolithic lithium disilicate posterior restorations after 5, 10, and 15 years: a retrospective case series. Int J Prosthodont. 2017;30(1):62-5. http://doi.org/10.11607/ijp.4997. PMid:28085983.
2. Meleka N, El-Banna A, El-Korashy D. Color stability and degree of conversion of amine-free dual cured resin cement used with two different translucencies of lithium disilicate ceramics. Braz Dent Sci. 2023;26(2):e3614. http://doi.org/10.4322/bds.2023.e3614.
3. Huettig F, Gehrke UP. Early complications and performance of 327 heat-pressed lithium disilicate crowns up to five years. J Adv Prosthodont. 2016;8(3):194-200. http://doi.org/10.4047/jap.2016.8.3.194. PMid:27350853.
4. Makhija SK, Lawson NC, Gilbert GH, Litaker MS, McClelland JA, Louis DR, et al. Dentist material selection for single-unit crowns: findings from the National Dental Practice-Based Research Network. J Dent. 2016;55:40-7. http://doi.org/10.1016/j.jdent.2016.09.010. PMid:27693778.
5. Mounajjed R, Layton D, Azar B. The marginal fit of E.max Press and E.max CAD lithium disilicate restorations: a critical review. Dent Mater J. 2016;35(6):835-44. http://doi.org/10.4012/dmj.2016-008. PMid:27546857.
6. Abd El-Moniem H, El-Etreby A, Salah T. Color and translucency of repressed lithium disilicate glass ceramic subjected to multiple firings and aging: color and translucency of ceramics. Braz Dent Sci. 2022;25(3):e3226. http://doi.org/10.4322/bds.2022.e3226.
7. Schweiger M, Höland W, Frank M, Drescher H, Rheinberger V. IPS Empress 2: a new pressable high-strength glass-ceramic for esthetic all-ceramic restorations. Quintessence Dent Technol. 1999;22:143-51.
8. Ivoclar [Internet]. 2017 [cited 2024 apr 27]. Available from: https://www.ivoclarvivadent.com/en_US/downloadcenter/?dc=us&lang=en#search-info-212=106005%2C1&search-info-210=106203%2C1&details=15136
9. Li RW, Chow TW, Matinlinna JP. Ceramic dental biomaterials and CAD/CAM technology: state of the art. J Prosthodont Res. 2014;58(4):208-16. http://doi.org/10.1016/j.jpor.2014.07.003. PMid:25172234.
10. Google [Internet]. 2024 [cited 2024 apr 27]. Available from: lang=en#search-info-210=106202%2C1&search-info-211=279006%2C1&search-info-212=106007%2C1&details=4857
11. Dental Products Report [Internet]. 2024 [cited 2024 apr 27]. Available from: https://www.dentalproductsreport.com
12. Garling A, Sasse M, Becker MEE, Kern M. Fifteen-year outcome of three-unit fixed dental prostheses made from monolithic lithium disilicate ceramic. J Dent. 2019;89:103178. http://doi.org/10.1016/j.jdent.2019.08.001. PMid:31394121.
13. Ortiz AL, Borrero-Lopez O, Guiberteau F, Zhang Y. Microstructural development during heat treatment of a commercially available dental-grade lithium disilicate glass-ceramic. Dent Mater. 2019;35(5):697-708. http://doi.org/10.1016/j.dental.2019.02.011. PMid:30827800.
14. Ortiz AL, Rodrigues CS, Guiberteau F, Zhang Y. Microstructural development during crystallization firing of a dental-grade nanostructured lithia-zirconia glass-ceramic. J Eur Ceram Soc. 2021;41(11):5728-39. http://doi.org/10.1016/j.jeurceramsoc.2021.04.036.
15. Zhang Y, Vardhaman S, Rodrigues CS, Lawn BR. A critical review of dental lithia-based glass-ceramics. J Dent Res. 2023;102(3):245-53. http://doi.org/10.1177/00220345221142755. PMid:36645131.
16. Phark JH, Duarte S Jr. Microstructural considerations for novel lithium disilicate glass ceramics: A review. J Esthet Restor Dent. 2022;34(1):92-103. http://doi.org/10.1111/jerd.12864. PMid:34995008.
17. Miranda JS, Barcellos ASP, Campos TMB, Cesar PF, Amaral M, Kimpara ET. Effect of repeated firings and staining on themechanical behavior and composition of lithiumdisilicate. Dent Mater. 2020;36(5):e149-57. PMid:32061444.
18. Gorman CM, Horgan K, Dollard RP, Stanton KT. Effects of repeated processing on the strength and microstructure of a heat-pressed dental ceramic. J Prosthet Dent. 2014;112(6):1370-6. http://doi.org/10.1016/j.prosdent.2014.06.015. PMid:25258270.
19. Gozneli R, Kazazoglu E, Ozkan K. Effects of repeated firings on colour of leucite and lithium di-silicate ceramics. Balkan Journal of Stomatology. 2013;17(3):122-7.
20. Cho SH, Nagy WW, Goodman JT, Solomon E, Koike M. The effect of multiple firings on the marginal integrity of pressable ceramic single crowns. J Prosthet Dent. 2012;107(1):17-23. http://doi.org/10.1016/S0022-3913(12)60011-0. PMid:22230912.
21. Aurélio IL, Dorneles LS, May LG. Extended glaze firing on ceramics for hard machining: crack healing, residual stresses, optical and microstructural aspects. Dent Mater. 2017;33(2):226-40. http://doi.org/10.1016/j.dental.2016.12.002. PMid:28069245.
22. Aurelio IL, Fraga S, Dorneles LS, Bottino MA, May LG. Extended glaze firing improves flexural strength of a glass ceramic. Dent Mater. 2015;31(12):e316-24. http://doi.org/10.1016/j.dental.2015.10.012. PMid:26599302.
23. Miranda JS, Barcellos ASP, Martinelli Lobo CM, Caneppele TMF, Amaral M, Kimpara ET. Effect of staining and repeated firing on the surface and optical properties of lithium disilicate. J Esthet Restor Dent. 2020;32(1):113-8. http://doi.org/10.1111/jerd.12558. PMid:31854512.
24. GC America Inc. [Internet]. 2024 [cited 2024 apr 27]. Available from: https://www.gc.dental/america/products/digital/gc_initial_lisi_block/GCA_Initial_LiSi_ Block_Brochure-digital.pdf
25. Straumann. Straumann® n!ce® Glass-Ceramic nice to meet you [Internet]. 2019 [cited 2024 apr 27]. Available from: https://www.straumann.com/content/dam/media-center/straumann/en/documents/brochure/product-information/490.396-en_low.pdf
26. Saint-Jean SJ. Dental glasses and glass-ceramics. In: Shen JZ, editor. Advanced ceramics for dentistry. Netherlands: Elsevier; 2014. p. 255-77.
27. HASSBio [Internet]. 2024 [cited 2024 apr 27]. Available from: https://www.hassbio.com/common/download.php?fullpath=board/14/364_0.pdf&filename=%5BEN%5D+Amber+Mill_Manual_English.pdf
28. VITA Ambria [Internet]. 2024 [cited 2024 apr 27]. Available from: https://mam.vita-zahnfabrik.com/portal/ecms_mdb_download.php?id=100097&sprache=en&fallback=de&cls_session_id=&neuste_version=1
29. Google [Internet]. 2024 [cited 2024 apr 27]. Available from: https://id=94347&sprache=en&fallback=de&cls_session_id=&neuste_version=1

30. Li S, Pang L, Yao J. The effects of firing numbers on the opening total pore volume, translucency parameter and color of dental all-ceramic systems. Hua Xi Kou Qiang Yi Xue Za Zhi. 2012;30(4):417-9. PMid:22934503.

31. Gonuldas F, Yilmaz K, Ozturk C. The effect of repeated firings on the color change and surface roughness of dental ceramics. J Adv Prosthodont. 2014;6(4):309-16. http://doi.org/10.4047/jap.2014.6.4.309. PMid:25177475.

32. Haag P. Porcelain veneering of titanium: clinical and technical aspects. Malmö: Faculty of Odontology, Malmö University; 2011.

33. Haag P, Ciber E, Derand T. Firing temperature accuracy of four dental furnaces. Swed Dent J. 2011;35(1):25-31. PMid:21591597.

34. Vichi A, Ferrari M, Davidson CL. Influence of ceramic and cement thickness on the masking of various types of opaque posts. J Prosthet Dent. 2000;83(4):412-7. http://doi.org/10.1016/S0022-3913(00)70035-7. PMid:10756290.

35. Hallmann L, Ulmer P, Gerngross MD, Jetter J, Mintrone M, Lehmann F, et al. Properties of hot-pressed lithium silicate glass-ceramics. Dent Mater. 2019;35(5):713-29. http://doi.org/10.1016/j.dental.2019.02.027. PMid:30853210.

36. Spink LS, Rungruanganut P, Megremis S, Kelly JR. Comparison of an absolute and surrogate measure of relative translucency in dental ceramics. Dent Mater. 2013;29(6):702-7. http://doi.org/10.1016/j.dental.2013.03.021. PMid:23618557.

37. Schaefer O, Watts DC, Sigusch BW, Kuepper H, Guentsch A. Marginal and internal fit of pressed lithium disilicate partial crowns in vitro: a three-dimensional analysis of accuracy and reproducibility. Dent Mater. 2012;28(3):320-6. http://doi.org/10.1016/j.dental.2011.12.008. PMid:22265824.

38. Fabian Fonzar R, Carrabba M, Sedda M, Ferrari M, Goracci C, Vichi A. Flexural resistance of heat-pressed and CAD-CAM lithium disilicate with different translucencies. Dent Mater. 2017;33(1):63-70. http://doi.org/10.1016/j.dental.2016.10.005. PMid:27855994.

39. Ohashi K, Kameyama Y, Wada Y, Midono T, Miyake K, Kunzelmann K-H, et al. Evaluation and comparison of the characteristics of three pressable lithium disilicate glass ceramic materials. Int J Dev Res. 2017;7:16711-6.

40. Yan ZL, Xian SQ, Tan T, Liao YM, Yang XY. Influence of zirconia content on translucency of zirconia-toughened alumina glass-infiltrated ceramic. West China Journal of Stomatology. 2011;29(2):191. PMid:21598497.

41. Nejatidanesh F, Azadbakht K, Savabi O, Sharifi M, Shirani M. Effect of repeated firing on the translucency of CAD-CAM monolithic glass-ceramics. J Prosthet Dent. 2020;123(3):530.e1. http://doi.org/10.1016/j.prosdent.2019.10.028. PMid:31916977.

42. Gaidarji B, Perez BG, Ruiz-Lopez J, Perez MM, Durand LB. Effectiveness and color stability of bleaching techniques on blood-stained teeth: an in vitro study. J Esthet Restor Dent. 2022;34(2):342-50. http://doi.org/10.1111/jerd.12850. PMid:34859941.

43. Wahba MM, Sherif AH, El-Etreby AS, Morsi TS. The effect of different surface treatments on color and translucency of bilayered translucent nano-crystalline zirconia before and after accelerated aging. Braz Dent Sci. 2019;22(2):203-12. http://doi.org/10.14295/bds.2019.v22i2.1622.

44. Dong-Dong Q, Lei Z, Xiaoping L, Wenli C. Effect of repeated sintering on the color and translucency of dental lithium disilicate-based glass ceramic. Hua Xi Kou Qiang Yi Xue Za Zhi. 2015;33(1):50-3. PMid:25872299.

45. Cho MS, Lee YK, Lim BS, Lim YJ. Changes in optical properties of enamel porcelain after repeated external staining. J Prosthet Dent. 2006;95(6):437-43. http://doi.org/10.1016/j.prosdent.2006.04.002. PMid:16765156.

46. El-Khayat H, Katamish H, El-Etreby A, Aboushahba M. Effect of varying thickness and artificial aging on color and translucency of cubic zirconia and lithium disilicate ceramics. Braz Dent Sci. 2021;24(3):1-9. http://doi.org/10.14295/bds.2021.v24i3.2623.

47. Pires-de-Souza FCP, Casemiro LA, Garcia LFR, Cruvinel DR. Color stability of dental ceramics submitted to artificial accelerated aging after repeated firings. J Prosthet Dent. 2009;101(1):13-8. http://doi.org/10.1016/S0022-3913(08)60282-6. PMid:19105987.

Iman Haggag Elnagar Ahmed
(Corresponding address)
October 6 University, Faculty of Dentistry, Fixed Prosthodontics,
Cairo, Egypt
Email: memohaggag93@gmail.com

Date submitted: 2024 Apr 27
Accept submission: 2024 May 27